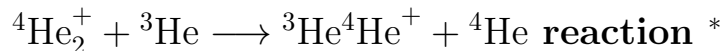


# Isotopic replacement in ionic systems: the



Enrico Bodo, Manuel Lara,<sup>†</sup> and Franco A. Gianturco<sup>‡</sup>

*Department of Chemistry, University of Rome La Sapienza,*

*Piazzale A. Moro 5, 00185 Rome, Italy*

## Abstract

Full quantum dynamics calculations have been carried out for the ionic reaction  ${}^4\text{He}_2^+ + {}^3\text{He}$  and state-to-state reactive probabilities have been obtained using both a time-dependent (TD) and a time-independent (TI) approach. An accurate ab-initio potential energy surface has been employed for the present quantum dynamics and the two sets of results are shown to be in agreement with each other. The results for zero total angular momentum suggest a marked presence of atom exchange (isotopic replacement) reaction with probabilities as high as 60%. The reaction probabilities are only weakly dependent on the initial vibrational state of the reactants while they are slightly more sensitive to the degree of rotational excitation. A brief discussion of the results for selected higher total angular momentum values is also presented, while the  $l$ -shifting approximation [1] has been used to provide estimates of the total reaction rates for the title process. Such rates are found to be large enough to possibly become experimentally accessible.

---

\* This work is affectionally dedicated to Prof. Volker Staemmler on the occasion of his 65th birthday: to a dear friend, an articulate scientist and a great scholar of  $\text{He}^+$ -containing systems.

<sup>†</sup>Present address: JILA, University of Colorado, UBC 440, Boulder CO., 80309 USA

<sup>‡</sup>Corresponding author: Dep. of Chemistry, University of Rome “La Sapienza”, P. A. Moro 5, 00185, Rome, Italy. Fax: +39-06-49913305. ; Electronic address: fa.gianturco@caspur.it

## I. INTRODUCTION

The study of helium nanodroplets has been shown over recent years to provide a very interesting and novel medium that acts as a "quantum matrix" in which one can probe the ro-vibrational and electronic spectroscopy of the various dopants which can be "solvated" in it and in which one can also observe the nonclassical effects caused by the surrounding He atoms [2, 3], together with the changes due to their bosonic/fermionic symmetry properties [4]. The experiments which can perform ionization of the helium matrix further raise the issue of the mechanism leading to ionization vs fluorescence, and of the understanding of the features of the interaction of the resulting ion with the atoms in the droplet which can show evidence of marked quantum many-body effects [5, 6].

One of the nanoscopic consequences of the formation of a permanent cationic impurity within the droplet is its high mobility within the weakly interacting solvent, whereby the positive charge can in principle migrate within it by some resonant charge hopping mechanism [7]. This process is taken to be terminated either by formation of a strongly bound  $\text{He}_2^+$  ion or by charge transfer to a dopant species. Our recent calculations on that process [8, 9] have shown that termination can also be achieved by multiple inelastic collisions within the droplet that enhance the evaporation of atoms from the latter. Furthermore, possible branching reactions of either the dopant ions or of the ionic moiety  $\text{He}_2^+$  could also occur within the droplet because either species will trend to move towards the center of the cluster in order to minimize the total potential energy of the composite system [11].

Recent experiments have been carried out on specific reactions initiated by primary ionization of the droplet [12, 13] and have shown that a rapid quenching of the internal degrees of freedom of the partner species is favored by the superfluid environment. The corresponding reactive branching of the ionic partners is therefore also markedly affected and could cause, in some cases, stabilization of intermediate complexes different from those expected, and seen, in the gas phase [13]. In a recent theoretical and computational study [14] we have in fact shown the possibility of having strongly exothermic chemical reactions without activation barrier, the occurrence of which should be greatly facilitated by the presence of the inert, quantum environment at the low temperatures existing within the helium "nanocryostat" [14].

In the present analysis we therefore wish to present calculations where the stabilized

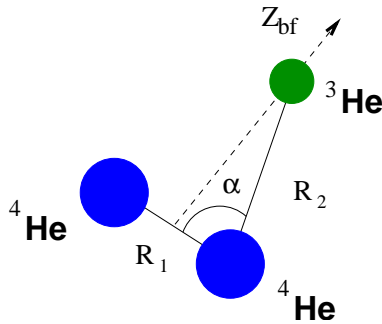


FIG. 1: Coordinates used in the TD code

primary ion in the droplet, the  $\text{He}_2^+$  species occupying its lowest ro-vibrational level, is made to react with one of the adatoms of the environment. The idea is to analyze several aspects of the problem which carry considerable theoretical interest and which can also guide us to understand the possible behavior of the ionized droplet under actual experimental conditions.

In particular, taking advantage of our recent calculations of the potential energy surface (PES) for the  $\text{He}_2^+ + \text{He}$  system [9], we have studied the quantum reaction for the isotopic exchange, i.e. for the molecule  $^4\text{He}_2^+$  colliding with neutral  $^3\text{He}$ , in order to add physical distinguishability within the process at hand. We have carried out the calculations, as we shall further describe below, using both a quantum time independent (TI) approach and a quantum, time dependent (TD) wavepacket approach. As we shall see, both methods produce essentially the same results and therefore provide a sort of internal check for our findings thereby adding further credibility to the present theoretical "experiments".

## II. THE TD CALCULATIONS

In the  $^3\text{He} + ^4\text{He}_2^+(v, j)$  collisional event two identical bosons  $^4\text{He}(S=0)$  forming a diatomic ion collide with a different isotope (fermion)  $^3\text{He}$  giving rise to inelastic ( $\rightarrow ^3\text{He} + ^4\text{He}_2^+(v', j')$ ) and reactive ( $\rightarrow ^4\text{He} + ^3\text{He}^4\text{He}^+(v', j')$ ) processes.

In a Body-Fixed (BF) frame of reference defined with respect to the Laboratory frame by the three Euler angles  $\theta, \phi, \chi$ , we have chosen to use bond coordinates as the three internal coordinates describing the relative position of the three particles (see Figure 1) that is two atomic distances  $R_1, R_2$  and the angle  $\alpha$  between them. A method based on these coordinates was presented previously and applied to the calculation of state-to-state reaction

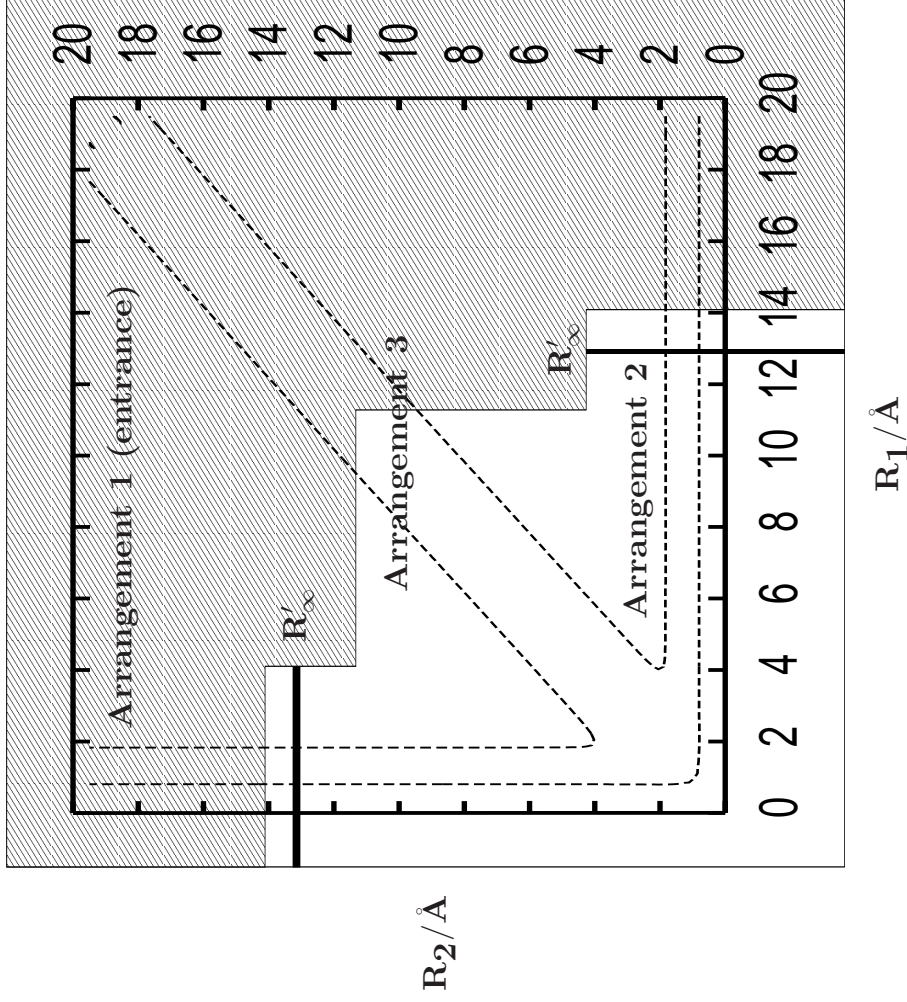
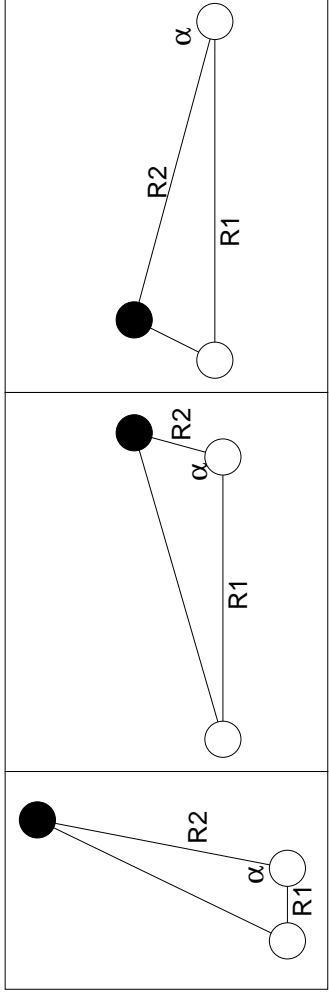


FIG. 2: Possible arrangements in the  $\text{He}_3^+$  (upper panel) system and their appearance on the PES of the complex (lower panel). See main text for details.

probabilities for the benchmark collision  $\text{Li} + \text{HF}$ [10]. It was shown there that its use may present certain advantages over the more commonly used Jacobi coordinates approach, for example when dealing with insertion reactions, thus making the bond coordinate approach method a viable and competitive alternative. One of the bottlenecks, in terms of computational costs of TD methods, is represented by the calculation of state-to-state reaction

probabilities because they would require relatively complicated changes of coordinates. Our present choice of bond coordinates allows a relatively simple and fast evaluation of these state-resolved probabilities when only two molecular arrangements are accessible of the three which exist in a generic ABC system. The method is applied here for the first time to a case in which all the three arrangements are open but where we can still exploit the AB<sub>2</sub> symmetry for the calculation of state-to-state probabilities, as we shall further explain later in this section.

A convenient BF frame is the one defined such that the  $z$ -axis lies along the vector joining the center of mass of the initial diatom to the <sup>3</sup>He atom (see Fig. 1) and the three atoms are in the  $xz$  plane. In the chosen set of coordinates  $(\theta, \phi, \chi, R_1, R_2, \alpha)$ , the complete Hamiltonian for an arbitrary value of the total angular momentum  $J$  takes the form[10]

$$H = -\frac{\hbar^2}{2\mu_1} \left( \frac{1}{R_1^2} \frac{\partial}{\partial R_1} R_1^2 \frac{\partial}{\partial R_1} \right) - \frac{\hbar^2}{2\mu_2} \left( \frac{1}{R_2^2} \frac{\partial}{\partial R_2} R_2^2 \frac{\partial}{\partial R_2} \right) + \left( \frac{1}{2\mu_1 R_1^2} + \frac{1}{2\mu_2 R_2^2} \right) \hat{\mathbf{L}}^2 + \frac{(\hat{\mathbf{J}}^2 - 2\hat{\mathbf{J}} \cdot \hat{\mathbf{j}})}{2\mu R^2} + \hat{T}_{12} + V(R_1, R_2, \alpha) \quad (1)$$

where we denote by  $m_0$ ,  $m_1$  and  $m_2$  the nuclear masses, with  $m_0$  being that of the "reference" atom, hence  $\mu_1 = m_0 m_1 / (m_0 + m_1)$ ,  $\mu_2 = m_0 m_2 / (m_0 + m_2)$  are the reduced masses associated with  $\mathbf{R}_1$  and  $\mathbf{R}_2$ , while  $\mu = m_2(m_0 + m_1) / (m_0 + m_1 + m_2)$  is the reduced mass associated with the  $\mathbf{R}$  Jacobi vector.

In Eq.(1)  $\hat{\mathbf{L}}^2$  is the angular momentum operator given by the following expression:

$$\hat{\mathbf{L}}^2 = -\hbar^2 \left\{ \frac{1}{\sin \alpha} \frac{\partial}{\partial \alpha} \sin \alpha \frac{\partial}{\partial \alpha} + \frac{1}{\sin^2 \alpha} \frac{\partial^2}{\partial \chi^2} \right\}. \quad (2)$$

while  $\hat{\mathbf{J}}$  is the total angular momentum operator. The term  $(\hat{\mathbf{J}}^2 - 2\hat{\mathbf{J}} \cdot \hat{\mathbf{j}}) / 2\mu R^2$  where  $\hat{\mathbf{j}}$  is the angular momentum of the diatomic molecule in the reactants' Jacobi coordinates, incorporates the Coriolis couplings given by:

$$\hat{\mathbf{J}} \cdot \hat{\mathbf{j}} = -i\hbar \left\{ \left( \frac{qR_1}{R_2 \sin \alpha} - \cot \alpha \right) \hat{J}_x \frac{\partial}{\partial \chi} - qR_1 \sin \alpha \hat{J}_y \frac{\partial}{\partial R_2} + \left( 1 - \frac{qR_1 \cos \alpha}{R_2} \right) \hat{J}_y \frac{\partial}{\partial \alpha} + \hat{J}_z \frac{\partial}{\partial \chi} \right\} \quad (3)$$

where  $q = \mu_1 / m_0$ .

Finally, in Eq. (1)  $\hat{T}_{12}$  is the kinetic energy cross term due to the non-Jacobian character

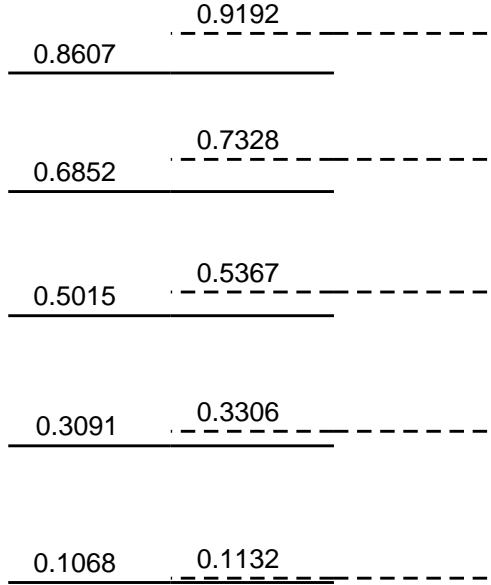


FIG. 3: Lowest ro-vibrational levels of the  $^4\text{He}-^4\text{He}$  (left) and  $^3\text{He}-^4\text{He}$ (right) molecules. For the former we have reported only the  $j = 1$  levels while for the latter we include only the  $j = 0$ . Energies are in eV, measured for the bottom of the entrance valley of reaction

of the internal coordinates we have chosen and has the form

$$\hat{T}_{12} = \frac{\hbar^2}{m_0} \left\{ \frac{\sin \alpha}{R_1 R_2} \frac{\partial}{\partial \alpha} - \cos \alpha \frac{\partial^2}{\partial R_1 \partial R_2} + \frac{\sin \alpha}{R_2} \frac{\partial^2}{\partial R_1 \partial \alpha} + \frac{\sin \alpha}{R_1} \frac{\partial^2}{\partial R_2 \partial \alpha} \right\} + \frac{\cos \alpha}{m_0 R_1 R_2} \hat{\mathbf{L}}^2 \quad (4)$$

When using the bond coordinates we can distinguish three regions in the PES associated with three different arrangements as described in figure 2: the entrance arrangement (that we shall call the channel 1)  $[\text{}^4\text{He}^4\text{He}]^+ + \text{}^3\text{He}$  and the two other possible product arrangements (2 and 3) that describe the  $[\text{}^4\text{He}^3\text{He}]^+ + \text{}^4\text{He}$  and  $[\text{}^3\text{He}^4\text{He}]^+ + \text{}^4\text{He}$  combinations. The arrangements 1 and 2 correspond respectively to coordinates  $R_1$  or  $R_2$  remaining finite while arrangement 3 would lie along the direction  $\alpha = 0$  as both  $R_1$  and  $R_2$  become very large. The inelastic process will be associated with the species remaining in channel 1, while both channels 2 and 3 will correspond to the reactive process: although, apparently treated in a very different way due to our system of coordinates, these two channels are physically equivalent.

## A. Wavepacket representation

The total wavepacket is, in the general case, expanded as[10]

$$\Psi^{JM\epsilon}(\theta, \phi, \chi, R_1, R_2, \alpha, t) = \sum_{\Omega \geq 0}^J W_{M\Omega}^{J\epsilon}(\phi, \theta, \chi) \frac{\Phi_{\Omega}^{JM\epsilon}(R_1, R_2, \alpha, t)}{R_1 R_2} \quad (5)$$

where  $W_{M\Omega}^{J\epsilon}$  are linear combinations of Wigner rotation matrices[15] of a given parity under inversion of all coordinates,  $\epsilon$ , and where  $M$  and  $\Omega$  are the projections of the total angular momentum,  $J$ , on the space-fixed (SF) and body fixed (BF)  $z$ -axis, respectively. Insertion of Eq.(5) into the time-dependent Schrödinger equation using the Hamiltonian of eq. (1), generally yields a set of first order differential equations for the  $\Phi_{\Omega}^{JM\epsilon}(R_1, R_2, \alpha, t)$  coefficients. For the case of  $J = 0$  which will be considered in the present calculations the previous expansion contains only one term. The wavefunction is then given by the solution of the equation

$$i\hbar \frac{\partial \Phi}{\partial t} = \left\{ -\frac{\hbar^2}{2\mu_1} \frac{\partial^2}{\partial R_1^2} - \frac{\hbar^2}{2\mu_2} \frac{\partial^2}{\partial R_2^2} + \left( \frac{1}{2\mu_1 R_1^2} + \frac{1}{2\mu_2 R_2^2} \right) \hat{\mathbf{I}}^2 + \hat{t}_{12} + V \right\} \Phi$$

with the following meaning of  $\mathbf{I}^2$  and  $\hat{t}_{12}$

$$\begin{aligned} \hat{\mathbf{I}}^2 &= -\hbar^2 \left( \frac{1}{\sin \alpha} \frac{\partial}{\partial \alpha} \sin \alpha \frac{\partial}{\partial \alpha} \right) \\ \hat{t}_{12} &= \frac{\hbar^2}{m_0} \left[ \sin \alpha \frac{\partial}{\partial \alpha} \left( \frac{1}{R_1} \frac{\partial}{\partial R_2} + \frac{1}{R_2} \frac{\partial}{\partial R_1} + \frac{1}{R_1 R_2} \right) \right. \\ &\quad \left. + \cos \alpha \left( \frac{1}{R_1} \frac{\partial}{\partial R_2} + \frac{1}{R_2} \frac{\partial}{\partial R_1} - \frac{1}{R_1 R_2} - \frac{\partial^2}{\partial R_1 \partial R_2} \right) \right] - \frac{\cos \alpha}{m_0 R_1 R_2} \hat{\mathbf{I}}^2 \end{aligned} \quad (6)$$

The integration of the above equation was performed by using the Chebyshev method[16] and the  $\Phi(R_1, R_2, \alpha, t)$  coefficient is represented on finite grids for the internal coordinates  $R_1, R_2, \alpha$ . A set of equidistant points,  $R_1^i, R_2^j$ , was chosen for the rectangular bidimensional radial grid ( $n_1 \times n_2$ ), which allows the evaluation of the radial kinetic terms using Fast Fourier Transforms (FFT)[17]. For the angle  $\alpha$  a set of  $n_{\alpha}$  Gauss-Legendre quadrature points,  $\alpha^k$  (with weights  $\omega^k$ ), is used. Thus, the terms involving derivatives in  $\alpha$  are evaluated through a discrete variable representation (DVR) transformation which reduces the procedure to a simple multiplication of a matrix by a vector [18, 19, 20, 21, 22, 23]. The grid representation of the wavepacket is then given by

$$[\Phi]_{ijk} = \Phi(R_1^i, R_2^j, \alpha^k) \sqrt{\omega^k} \quad (7)$$

TABLE I: Parameters used in the wavepacket propagations for  $\nu = 0, 1, 2$   $j = 1$  and  $J = 0$ ; distances in Å, times in ps. The gaussian parameters  $(\mathcal{K}_0, \Gamma)$  in Eq (9), are given by (14.30, 0.42), (10.87, 0.55), (6.27, 0.96) respectively

$(R_1^{min}(\text{Å}), R_1^{max}(\text{Å}), n_1)$	0.69, 19.50, 360
$(R_2^{min}(\text{Å}), R_2^{max}(\text{Å}), n_2)$	0.69, 19.50, 360
$n_\alpha$	130
$(R_1^{abs}(\text{Å}), \Upsilon_1)$	14.10, 0.016
$(R_2^{abs}(\text{Å}), \Upsilon_2)$	14.10, 0.016
$(R_0(\text{Å}), R'_\infty(\text{Å}))$	13.00, 13.00
$\Delta t(ps)$	0.003

where, for convenience, the Gauss-Legendre weights are introduced.

In order to use a finite bidimensional radial grid, the wavepacket is absorbed at each time step by multiplying the wavepacket for  $f_1(R_1)f_2(R_2)$ , where  $f_i(R_i) = \exp[-\Upsilon_i(R_i - R_i^{abs})^2]$  for  $R_i > R_i^{abs}$  and  $f_i(R_i) = 1$  otherwise. The absorbing regions are presented in the lower panel of Figure 2 as a shaded area.

The actual parameters of the propagation used in the calculations are listed in Table I. It should be noted that the number of angles,  $n_\alpha$ , required to converge is indeed very large: channel 3 is asymptotically open only for  $\alpha = 0$  and many angular quadrature points are required in order to have a grid dense enough in the small-angle region. The initial wavepacket represents the reagents approaching the collision region with the diatom in a given  $(\nu, j)$  ro-vibrational state and with a continuum distribution of relative kinetic energies. The initial wave packet can thus be expressed (in reactants' Jacobi coordinates  $(r, R, \gamma)$ ) as a product of a diatomic wavefunction and a Gaussian function for the relative translational coordinate:

$$\Phi(t = 0) = \chi_{\nu j}(r)Y_{j\Omega_0}(\gamma, 0)G(R) \quad (8)$$

where  $G(R)$  is a complex Gaussian function written as follows

$$G(R) = \left(\frac{2}{\pi\Gamma^2}\right)^{1/4} \exp\left[-\frac{(R - R_0)^2}{\Gamma^2} - i\mathcal{K}_0(R - R_0)\right]. \quad (9)$$



The gaussian is centered at a convenient  $R_0$  value such that the interaction between the reactants can be considered negligible. The energy distribution for the initial wavepacket  $a(E)$  is then determined using

$$a(E) = \left( \frac{\mu}{2\pi\hbar^2 k_{\nu j}} \right)^{1/2} \int e^{ik_{\nu j}R} G(R) dR \quad (10)$$

with  $k_{\nu j} = \sqrt{2\mu(E - E_{\nu j})/\hbar^2}$ .

This system contains two identical bosons and hence the total wavefunction must obey the correct spin statistics: the total wavefunction must have the correct symmetry under the action of the  $P_{12}$  operator that exchanges the two bosons. This means that (as in all the AB<sub>2</sub> systems) the calculations with even and odd initial  $j$  values for the diatomic wavefunction are decoupled: since the Hamiltonian commutes with the parity operator  $P_{12}$ , a wavepacket built as an eigenfunction of  $P_{12}$  (as it occurs with our initial wavepacket  $\Phi(t = 0)$ ) will remain so under time evolution. An additional simplification in our calculations stems from the consideration that, since the  ${}^4\text{He}_2^+$  is a  $\Sigma_u^+$  molecule composed of two spinless nuclei, only odd rotational states are allowed in the entrance arrangement. As a consequence of these constraints, it is clear that the appearance of the forbidden even- $j$  rotational states in the inelastic distributions obtained from the evolved wavepacket using eq. (11) below would indicate convergence problems. This was one of the various criteria we used for checking convergence in our present calculation and we found no instance where such states would appear.

The main steps of the TD method applied to the  $J=0$  case were the following [10]:

- The initial wavepacket, obtained in the reactants' Jacobi coordinates  $(r, R, \gamma)$  is transformed into bond coordinates  $(R_1, R_2, \alpha)$ ;
- The propagation is performed using bond coordinates;
- The S matrix elements for the transition into any other reactive or inelastic final state can be obtained from the evolved wavepacket using the product asymptotic analysis method of Balint-Kurti *et al.* [24, 25] that requires a change of coordinates to the Jacobi system  $(R'_\infty, r', \gamma')$  corresponding to the final arrangement. From the transformed wavepacket at each time step, the state-to-state probabilities are obtained

using the expression

$$P_{\nu j \rightarrow \nu' j'}(E) = \frac{1}{|a(E)|^2} \frac{k_{\nu' j'}}{2\pi\mu} |A_{\nu' j'}(R'_\infty, E)|^2 \quad (11)$$

where, as noted above,  $k_{\nu' j'} = \sqrt{2\mu(E - E_{\nu' j'})}/\hbar$ ,  $\mu$  is the reduced mass of the desired arrangement channel,  $R'_\infty$  is a value of the Jacobi radial coordinate well into the asymptotic region and the  $A_{\nu' j'}(R'_\infty, E)$  are the energy transforms defined for the desired channel as:

$$A_{\nu' j'}(R'_\infty, E) = \int_0^\infty dt e^{iEt/\hbar} \langle \chi_{\nu' j'}(r') P_{j'0}(\cos \gamma') | \Phi(R'_\infty, r', \gamma', t) \rangle \quad (12)$$

The computational cost of the required coordinate transformations is not very high because the arrangement channels 1 and 2 share one of the Jacobi radial coordinates with the bond coordinates system  $r' = R_i$ , thereby reducing the numerical effort due to coordinates transformations: even in the general case of  $J \neq 0$ , only simple rotations on the plane identified by the three atoms would be required to move to the desired BF system. Arrangement 3 would require a much more expensive change of coordinates, but due to the symmetry, the probability for the  $^3\text{He}$  to strip either of the two  $^4\text{He}$  atoms must be exactly the same. Hence, we can assume that the probabilities in channel 3 are the same as those in channel 2 and thus we can avoid calculating them; any deviation from unity of the sum of all of them can then be taken as a sign of lack of convergence. This has been another criteria in determining the convergence of our calculations in the actual situations of this work.

## B. The TI Calculations

We have employed the *abc* program of Skouteris et al. [26] which performs an expansion of the total wavefunction in Delves hyperspherical coordinates [27] and uses the coupled channel method formulated by Schatz [28] with an additional orthogonalization scheme of the vibrational basis at fixed hyperradius to avoid over-completeness of the basis set in the short range region [29]. The coupled channels equations are then solved using the constant reference potential log-derivative algorithm of Manolopoulos [30].

The convergence of the resulting S matrix is sensitive to two parameters, the hyperradius  $\rho_{max}$  at which the asymptotic condition is imposed and the step-size  $\Delta\rho$  of the propagator.

Converged results within 1% were obtained with  $\Delta\rho=0.02$  a.u. and  $\rho_{max} = 25.0$  a.u. for the lowest collision energy considered here ( $\sim 7$  meV).

The basis set was built using all the ro-vibrational levels of the two  $[\text{He-He}]^+$  diatomics whose energies lie below the cut-off energy value of 1.5 eV as measured from the bottom of the entrance channel. Since our calculations would have otherwise involved the use of too many rotational levels, we have imposed a maximum value of  $j_{max}=20$  for each molecule which is enough to obtain probabilities converged within 5% also for the highest rotational states included. The basis set chosen has been able to reproduce almost perfectly the TD results also at the highest energies employed here as we shall see below. Our basis set comprised of a total of 235 basis functions for  $J = 0$ . As noticed before the  $[\text{}^4\text{He-}^4\text{He}]^+$  molecule can only have odd rotational states.

We have performed the calculations for about a thousand different collision energies on a grid ranging from 7.375 meV up to 1 eV. The lowest collision energy has been chosen to be 1 meV higher than the energy necessary to make the reactive channel for the title reaction to be energetically accessible when considered in the following direction



The small endothermicity of 6.375 meV is due to the difference of zero point energy between the  $\nu = 0, j = 1$  state of the reactants in eq. (13) and the  $\nu = 0, j = 0$  state of the heteronuclear product molecule. For clarity we report in Figure 3 a diagram of the vibrational energy levels involved in the calculations.

### III. RESULTS AND DISCUSSION

In Figure 4 we report the reaction probability when starting with the initial state ( $\nu = 0, j = 1$ ) and summing over all the final accessible states. The two sets of data that refer to the two different, independent calculations we have mentioned above are in good agreement over the whole energy region of interest and provide a useful internal check of our calculations. The small differences are due to different causes: first the truncated size of our basis set expansion in the TI code is the source of a small level of inaccuracy especially for the transitions involving the higher rovibrational states; in second place, the TD calculation become inaccurate (as expected in general) for very low kinetic energies (below

10 meV in the present case) because of the finite time for propagation that necessarily neglects the contribution to the correlation functions coming from longer times. The *abc* program uses in fact a basis set which is constructed as an orthogonalized product of ro-vibrational arrangement wavefunctions. As a consequence, the description of reactions where triangular geometries are dominant (e.g.  $\text{Li}_2+\text{Li}$  system) may be inaccurate. Although our system here has clearly shown a transition state and a minimum energy path that is mainly collinear [8, 9], we still intend to provide a consistency check of our calculations by comparing the TI results with those from a TD method that is not based on basis sets expansion. On the other hand, the TD method is based on a time propagation in bond coordinates and might therefore present some problems when applied to a  $\text{A-B}_2$  system where the third arrangement (channel 3 in Figure 2) becomes energetically accessible when  $\alpha \sim 0$ ; this would require many angular points in order to describe the reactive process as discussed earlier on in this work.

The pattern of resonances that can be seen in the reaction probabilities profile is very complicated as many of these features may be due to the opening of the various asymptotic channels of the two diatomics involved in the reaction. Many others are likely to be due to Feshbach-type resonances with metastable states of the triatom and to potential trapping due to centrifugal barriers in the exit channels, but it would be premature to analyze them now in any detail given the absence of some experimental indication as to their physical presence.

In Figure 5 we report the individual contributions of the reaction probabilities for different final vibrational channels (the probabilities are rotationally summed). As can be seen from that figure, the total reaction probability is larger than 60% over most of the range of collision energies considered here (the collision energy in this figure is measured with respect to the  $^4\text{He}_2(\nu = 0, j = 1)$  channel i.e. to the reactants' ground state). However, at large collision energies the probability of populating the ground vibrational state of the products decreases and the flux is more or less equally redistributed over all the open, final vibrational states.

In the highly symmetrical systems like  $\text{A}_3$  one should expect that the total reaction probabilities would be exactly the same as the non-reactive one simply because the two fluxes are not distinguishable. In our case, however, a certain degree of asymmetry is introduced by the isotopic change and therefore the reactive process becomes more likely to occur than the inelastic collision process. This feature, at high energies (above 1.0 eV) is

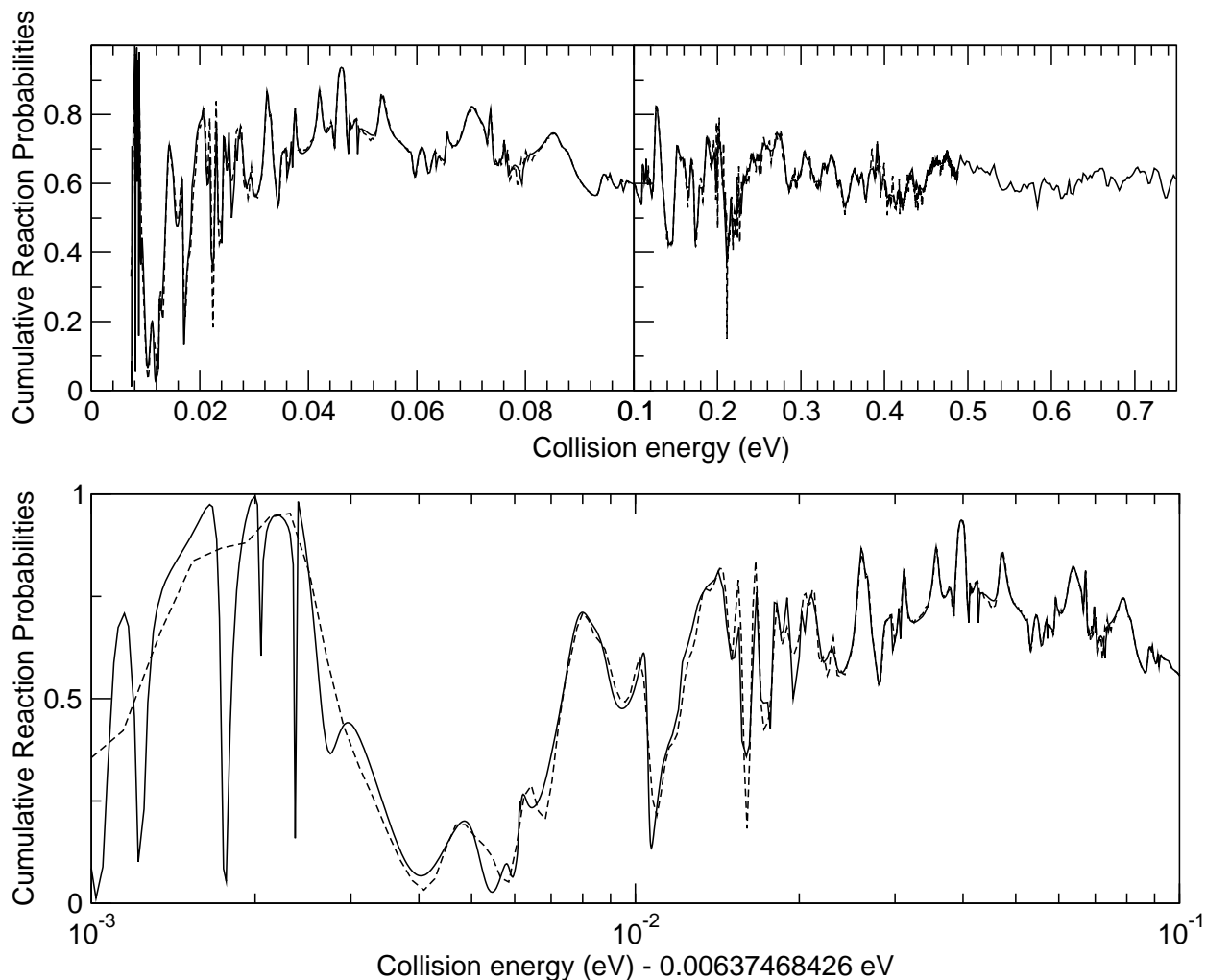


FIG. 4: Reaction probabilities for TD (dotted lines) and TI (solid lines) calculations for the initial state ( $\nu = 0, j = 0$ ). The lower panel shows the same probabilities on a logarithmic scale for the lowest energies above reaction threshold

however mainly due to the fact that there are two arrangements containing the product AB molecule. At these energies, in fact, the helium exchange reaction has a total probability of roughly 60%, 30% for each of the two possible exchange, while we find a 40% probability of simple elastic/inelastic non-reactive scattering. This behavior may be attributed to the mass difference because it seems reasonable that when the collision takes place at high energies the lighter  $^3\text{He}$  may be not efficient in substituting the heavier isotope. We also believe that, given the relatively high collision energies employed here, the small difference of zero point energy mentioned in the previous section has a very small effect on the dynamical behavior.

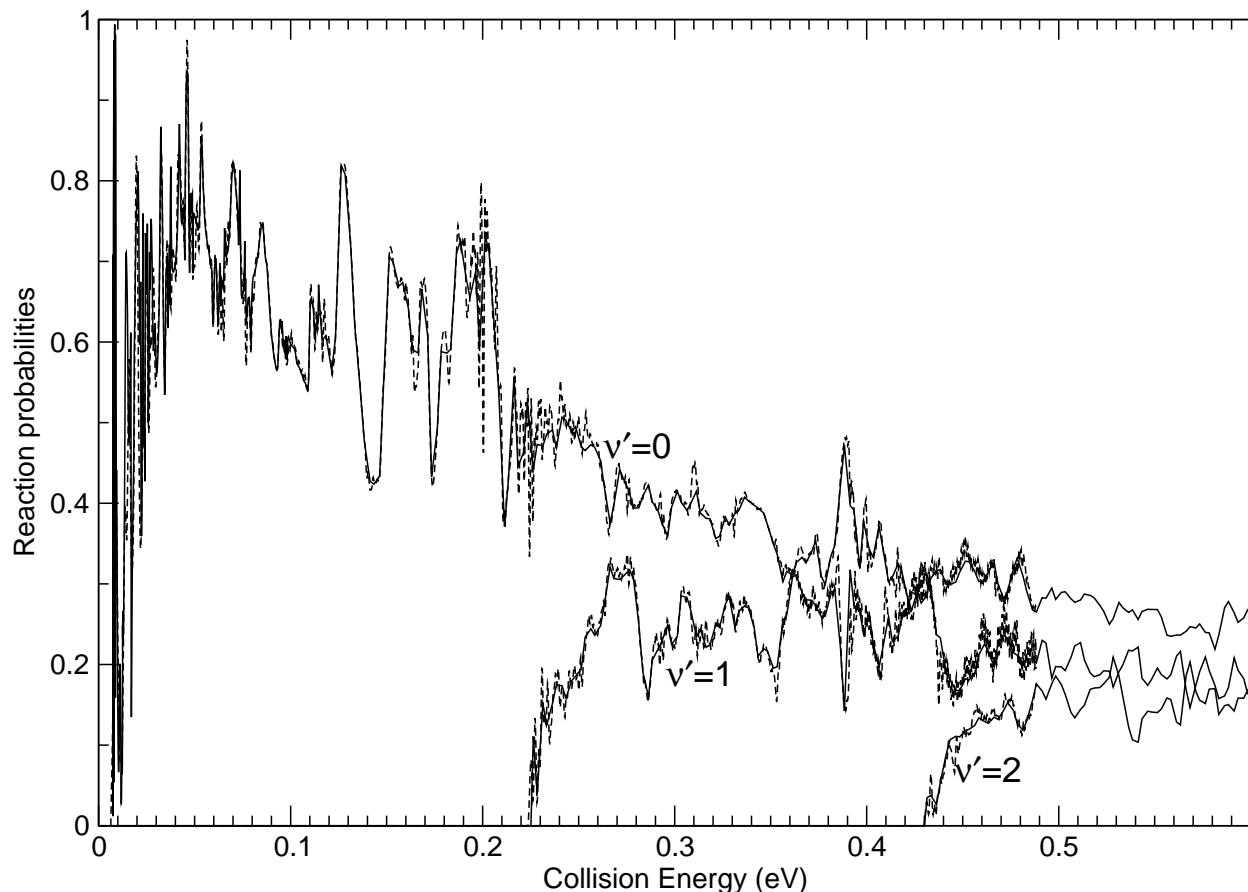


FIG. 5: TI (solid lines) and TD (dashed lines) rotationally summed reaction probabilities for different final vibrational states. The initial state of the reactant molecule is ( $\nu = 0, j = 0$ ).

Below 1.0 eV we see from Figure 4 that the probability may rise well above 0.6 and reaches the range 0.8-1. In this case the probability of a non-reactive scattering is less than 20%. We believe that the dominant effect at these lower energies may be the higher density of states of the product AB molecule with respect to the reactant  $A_2$  molecule which has only odd rotational states for the symmetry reasons mentioned before.

Much more difficult is the task of finding significant patterns of behavior in the final products' rotational distributions. The first three state-to-state reaction probabilities for different final rotational states, when the reaction begins with the ground state reactants are reported in Figure 6. We can immediately see there that high degree of variation of each individual probability persists as  $j$  changes as it also does for the other open channels not shown in the Figure. At higher energies (not shown in the Figure), on the other hand, the

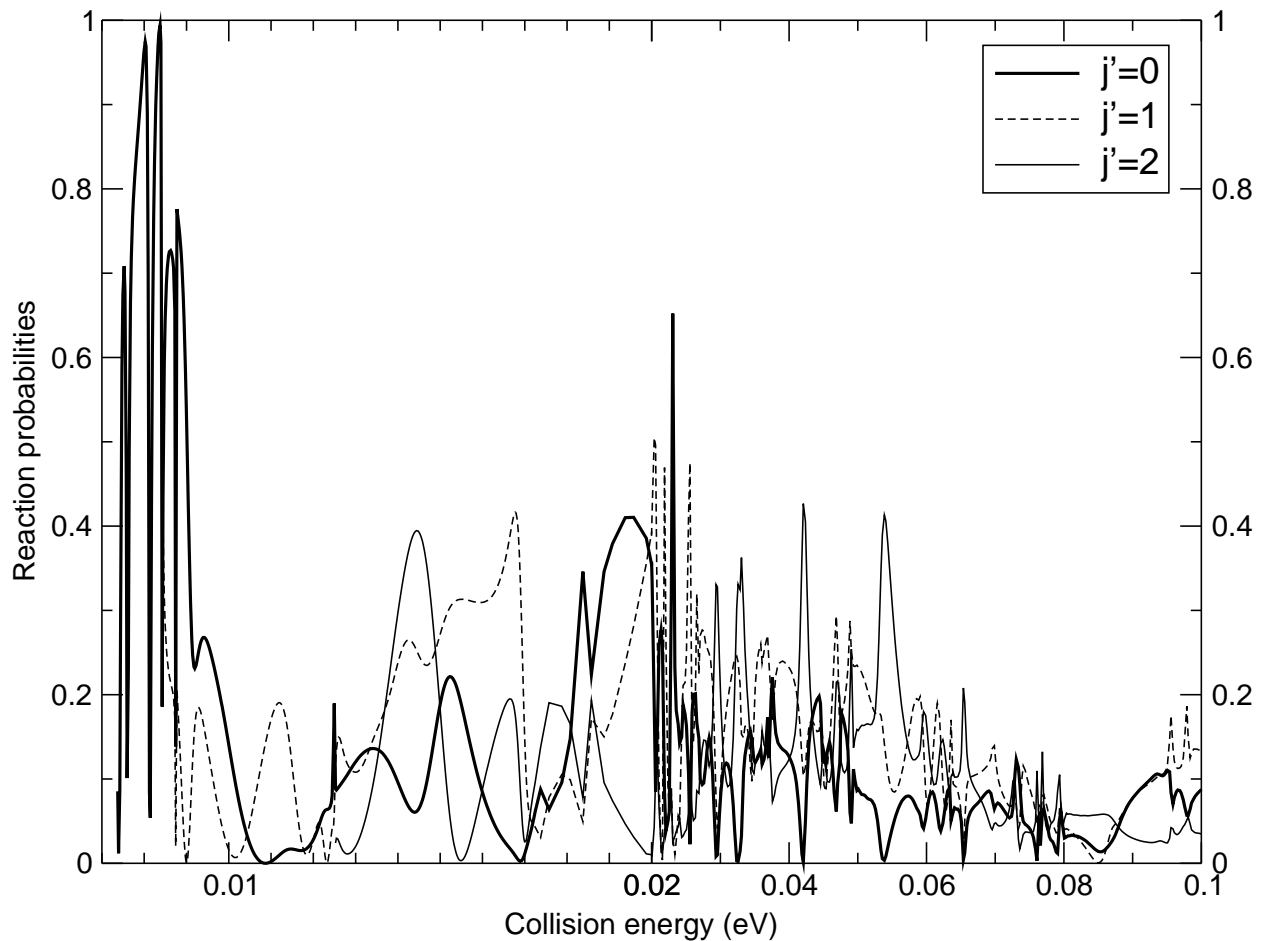


FIG. 6: A limited portion of the TI state-to-state reaction probabilities for ground state reactants and various final rotational states i.e. for the reaction  ${}^4\text{He}_2^+(\nu = 0, j = 0) + {}^3\text{He} \rightarrow {}^4\text{He}^3\text{He}^+(\nu = 0, j') + {}^4\text{He}$  where the final molecule is always in the  $\nu = 0$  vibrational level

various final rotational states of the product molecule are all substantially populated.

Another important piece of information that we may obtain from our calculations is the effect of increasing the internal energy (i.e. the ro-vibrational excitation) of the reactants. In Figure 7 we therefore report the total reaction probability summed over all the open final states but now for three different initial states ( $\nu = 0, j = 1$ ), ( $\nu = 1, j = 1$ ) and ( $\nu = 2, j = 1$ ) (the collision energies have been selected relative to the specified initial state). As it can be easily seen for this figure, the initial degree of vibrational excitation (at least for the lowest states examined here) does not change significantly the overall dynamical behavior of the system: the reaction probabilities rise rapidly at threshold from zero to  $\sim 60\%$  and remain roughly of that size when the collision energy increases.

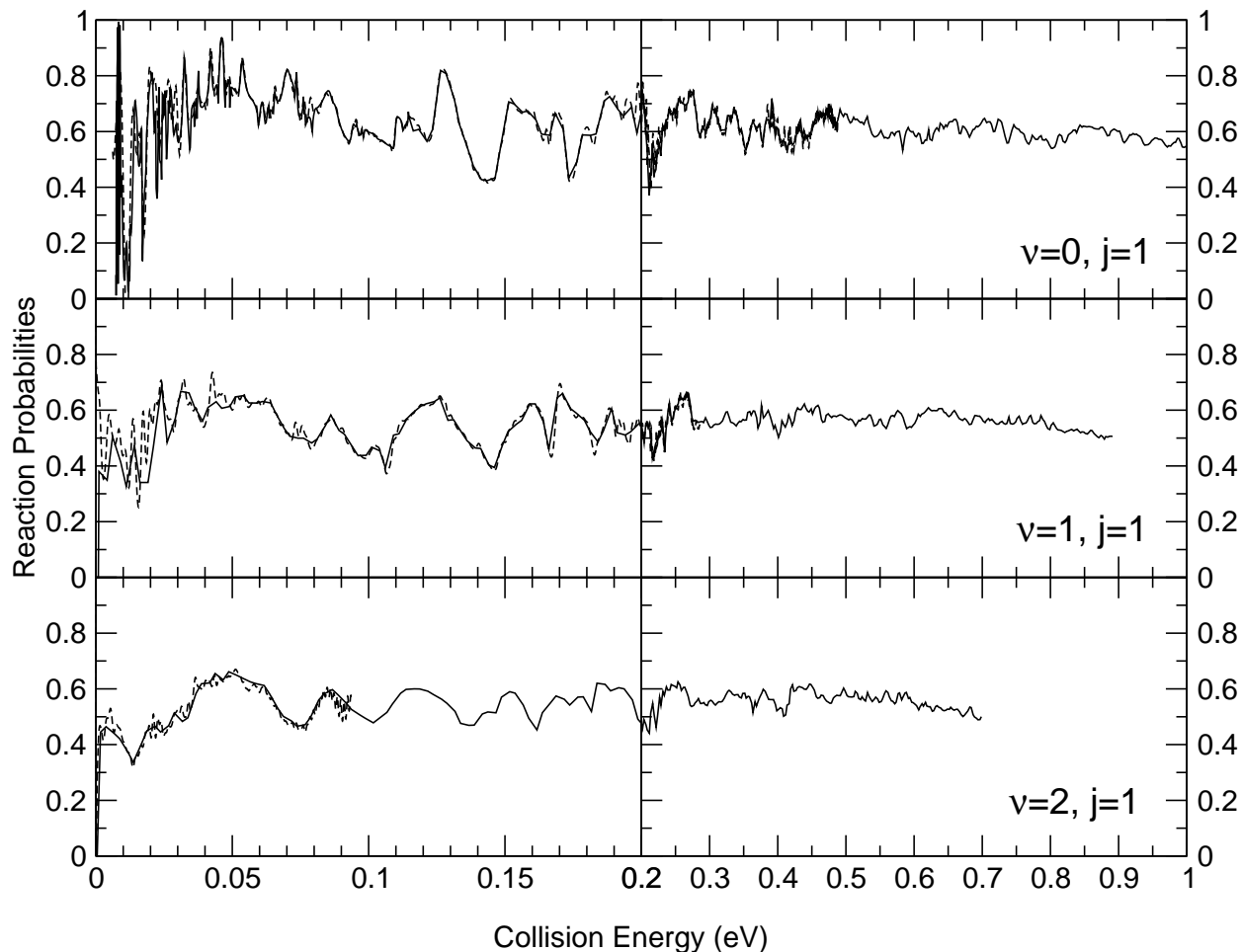


FIG. 7: TI reaction probabilities for different initial vibrational states (solid lines); TD results are also reported as dashed lines

A similar situation has been obtained when considering the reactions probabilities produced by rotationally excited reactants. For example when looking at the results reported in Figure 8 we see how even a large rotational energy content does not produce a corresponding increase in reaction probabilities. It is worth pointing out however that we are limiting this analysis to the  $J = 0$  case and therefore a situation in which the initial molecular angular momentum is balanced by a corresponding relative orbital angular momentum  $l$ . This means that the reaction paths that we sampled here with rotationally excited molecules would present centrifugal barriers. In conclusion, however, we can say that the reaction dynamics in our system is probably dominated by resonances and therefore the memory of the initial rotational state is soon lost during the reaction.



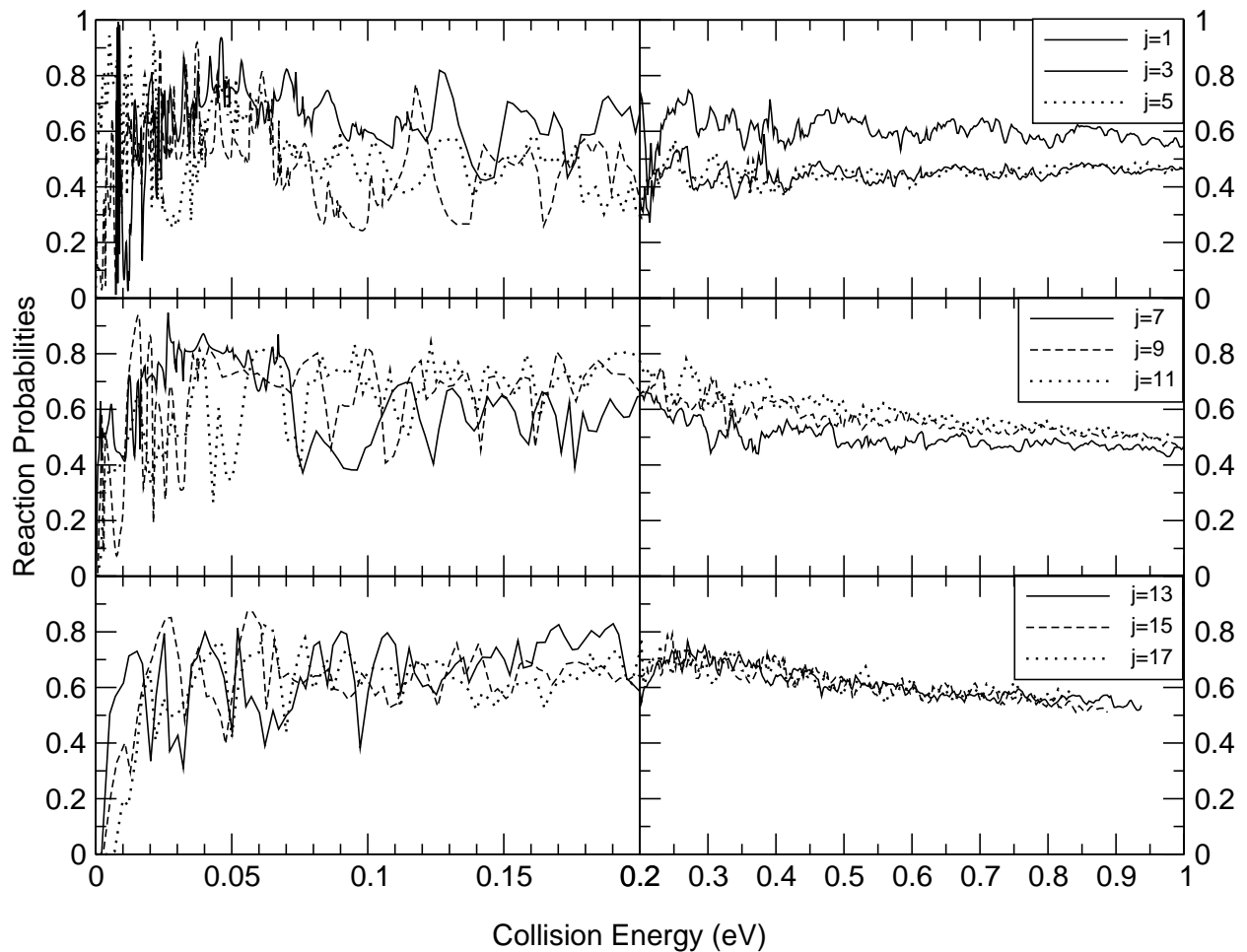


FIG. 8: TI reaction probabilities for different initial rotational states (the reactant molecule is in the  $\nu = 0$  vibrational state)

#### IV. HIGHER ANGULAR MOMENTA

To increase the value of the total angular momentum beyond  $J = 0$  for reactive scattering is still a computationally demanding task. From the analysis of the lower partial waves, however, we can already extract useful information about the overall dynamics. When going to the situation with  $J \neq 0$  the number of coupled channels increases due to the proliferation of the possible  $\Omega$  values, where  $\Omega$  is the helicity quantum number [26]. Furthermore, for each  $J > 0$  value we have two possible values of the total parity eigenvalues ( $p = \pm 1$ ) which require two independent calculations. The calculations for  $J \neq 0$  that we present here are "exact" (no approximations such as coupled states have been used) and have been done

using the TI method outlined above and the *abc* code.

We report in Figure 9 and 10 the total probabilities for  $J = 1$  and  $J = 2$  for the reaction which starts with  ${}^4\text{He}_2^+(\nu = 0, j = 1)$ . In both cases the results are compared with the  $J = 0$  reaction probabilities (thick solid lines in the upper panels). As can be seen in the upper panels of those figures the reaction probabilities for higher angular momenta are very similar to the ones for  $J = 0$ , the only difference being the small shifts in the resonance pattern. This is true also at relatively low energies although the resonance pattern is becoming different especially close to threshold.

When looking at the lower panels of Figs. 9 and 10 we can further see the contributions due to the initial  $\Omega = 1$  helicity component of the reaction: as it may be expected for a reaction which has a marked collinear constraint this last contribution is significantly lower than for  $\Omega = 0$  especially at lower energies.

Given the fact that accurate calculations for other values of  $J > 0$  would require computational times which are too long and since we are here in presence of a ionic potential which in principle may require many total  $J$  in order to properly converge to a reactive cross section, we have decided to calculate the reaction rate constants by using something similar to a  $J$ -shifting approximation, i.e. by using only the  $J = 0$  reaction probability  $P(E)$  to estimate the total rate constant. A realistic approximation when dealing with barrierless (ionic) systems like the one we are examining here, has been suggested in Ref [1]: this approximation essentially consists in obtaining the  $J \neq 0$  reaction probabilities by judiciously “shifting” the  $J = 0$  values. We have here used the formula:

$$P_J(E; \nu, j) \sim P_{J=0}(E - V_J^*; \nu, j) \quad (14)$$

where  $\nu, j$  identify the initial state of the reactants and  $V_J^*$  is the height of the centrifugal barrier of the entrance channel taken along a suitable monodimensional potential generated by a non-zero initial orbital angular momentum  $l$  value that is allowed for a given  $J$  and  $j$ ; we have chosen to use the potential of a collinear geometry given by  $\text{He} - r_{eq} - \text{He} - r - \text{He}$  with  $r_{eq} = 2.046$  a.u.. The only difference with ref. [1] is that we have initially a  $j = 1$  molecule which means that for each  $J$  value there are three allowed values of  $l$  given by  $|J - 1| \leq l \leq J + 1$ . Since this happens for all  $J$  values that may contribute, the further

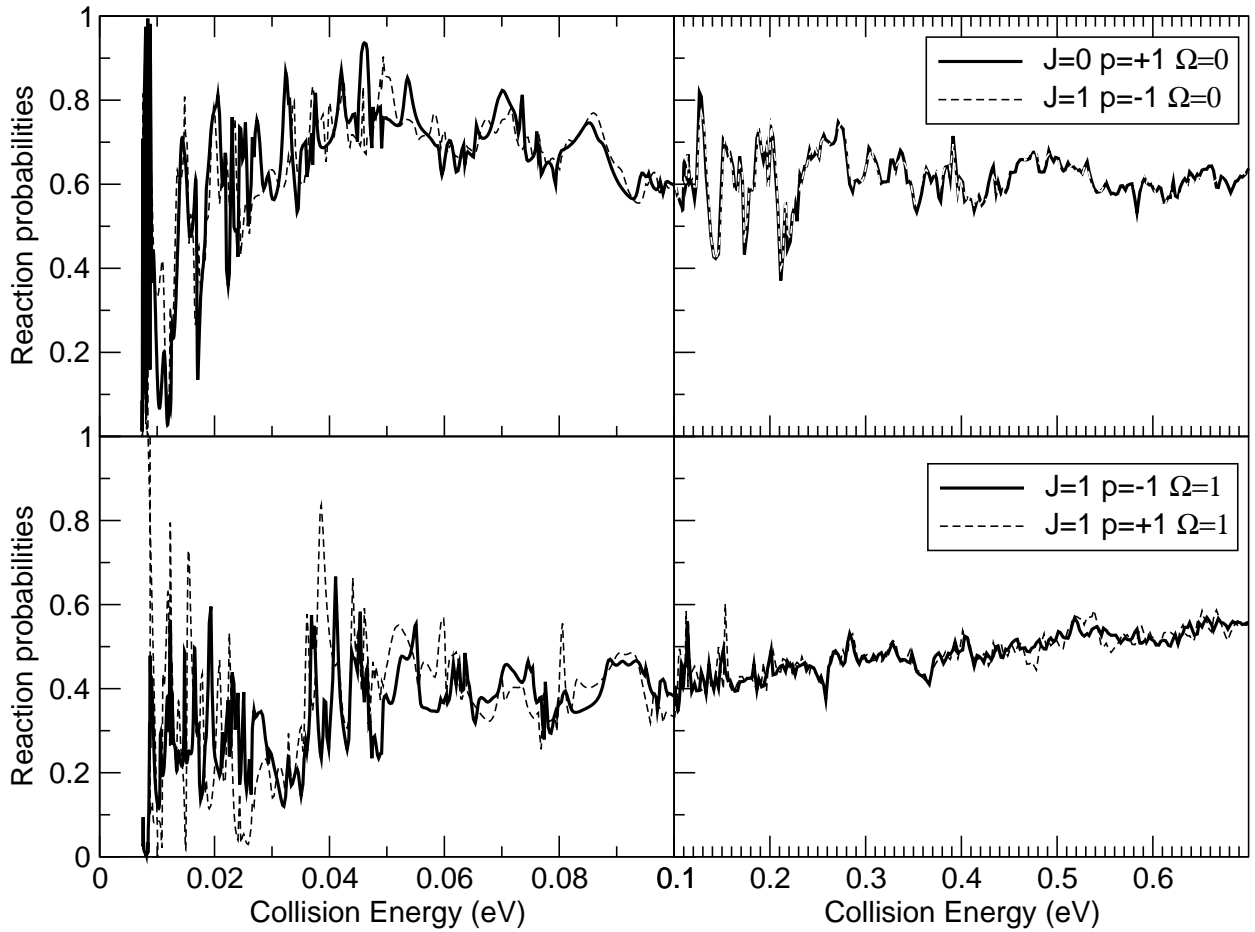


FIG. 9: TI reaction probabilities for  $J = 1$ ,  $\Omega = 0$  (upper panel) and for  $J = 1$ ,  $\Omega = 1$  (lower panel)

initial- $j$  averaging leaves the cross section unchanged

$$\sigma(E_{coll}; \nu, j) = \frac{\pi}{k_{coll}^2} \sum_J (2J + 1) P_J(E; \nu, j) \quad (15)$$

From this cross section we finally obtain the rate constants reported in Figure 11. Although this is a very approximate prescription, our final result can still tell us that the rate constant for a reactive exchange process in  $\text{He}_3^+$  is of the order of  $10^{-11} - 10^{-9} \text{ cm}^3 \cdot \text{s}^{-1}$  a value that is significantly lower than the Langevin capture rate also reported in Figure 11. One should note also that, although Langevin capture rates assume the reaction to be exoergic, the very small endoergicity of the present system still allows us to use it for an estimate of the reaction rates.

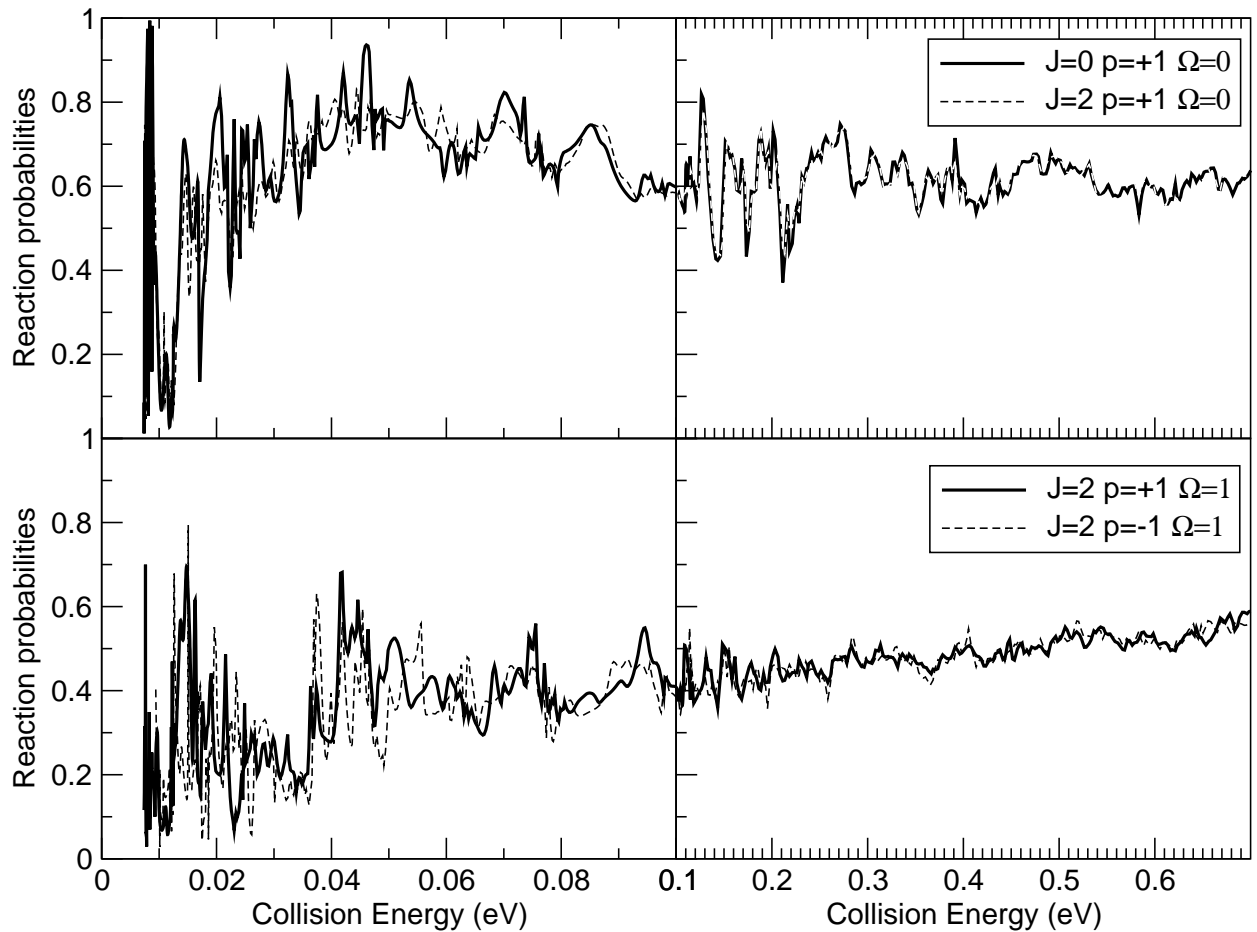


FIG. 10: TI reaction probabilities for  $J = 2$ ,  $\Omega = 0$  (upper panel) and for  $J = 2$ ,  $\Omega = 1$  (lower panel)

## V. PRESENT CONCLUSIONS

We have presented new theoretical results on the reactive dynamics of  $\text{He}_3^+$  system. In particular, we have discussed the reactive behavior for the lowest total angular momenta and have extended the calculations to obtain approximate rate constants for the title reaction. In order to make the process physically clearer and to get a better insight into its mechanism, we have substituted one of the  $^4\text{He}$  with an  $^3\text{He}$  so that we have introduced a small endothermicity in the atom exchange process that is occurring during the reactive event. In this way we have also introduced an asymmetry in the density of states associated with the reactants (here an homonuclear molecule) and the products (here an heteronuclear molecule). This difference makes for a more favorable reactive process with respect to

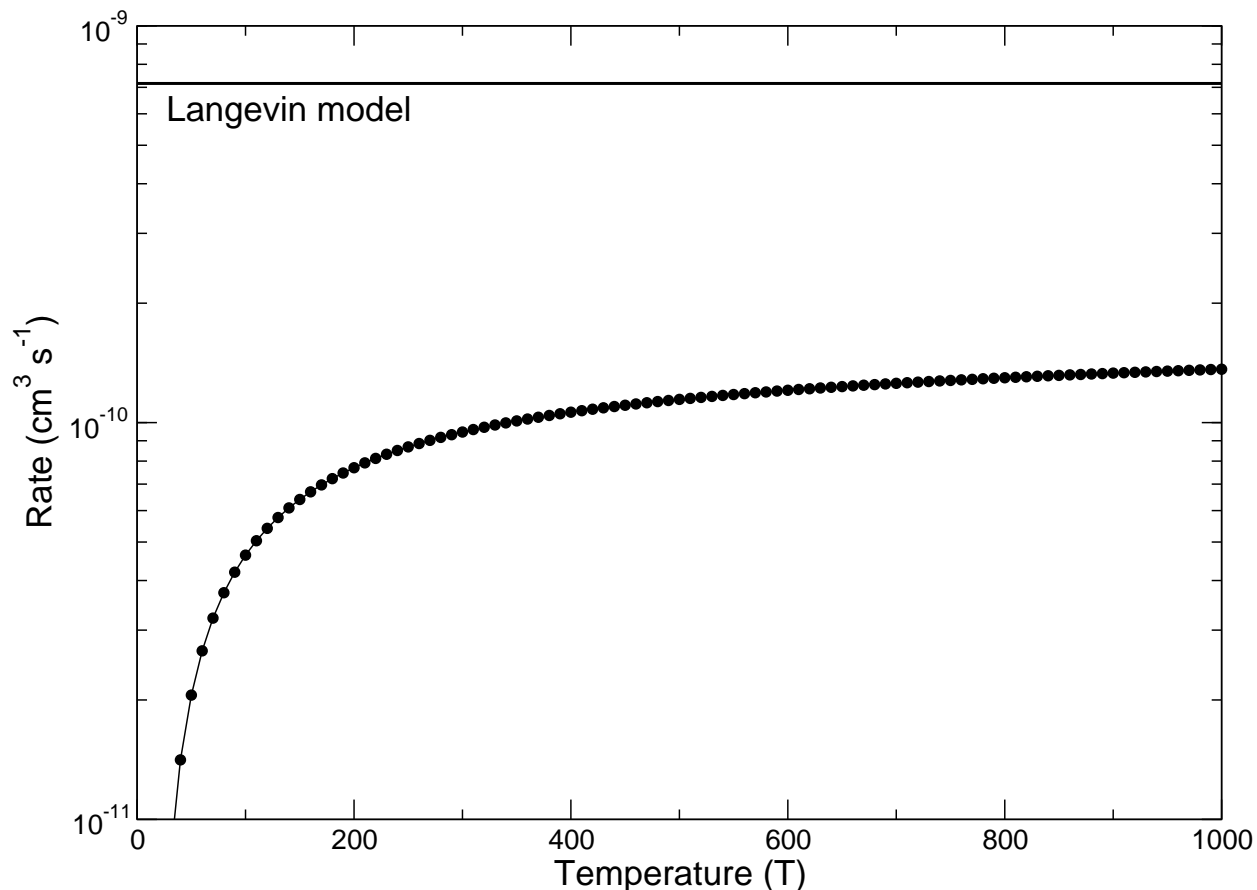


FIG. 11: Rate constants for the reaction  ${}^4\text{He}_2^+ + {}^3\text{He} \longrightarrow {}^3\text{He}{}^4\text{He}^+ + {}^4\text{He}$  as a function of temperature. Also shown as an horizontal line is the Langevin value.

the simpler inelastic collision process as shown by our calculations.

The reaction considered here has a collinear MEP without activation barrier and therefore behaves in the main like a typical ionic reaction. We have obtained complete state-to-state probabilities for the reaction using a time independent method and then, because there may be some issues related to the use of an arrangement-based basis set expansion, we have checked the numerical reliability of our TI findings by further reproducing our results using a time dependent procedure.

Our present results clearly show that the reaction under study turns out to be quite efficient when  $J = 0$  and represents more than 60% of the scattered flux at the energies considered. Internal excitation of the colliding partner does not appear to produce substantial increases of the reaction probabilities at least for the lowest vibrational and rotational states

of the reactants. Even with relatively highly rotationally excited  $\text{He}_2^+$  (up to  $j = 19$ ) the size of the reactive probability remains very similar to the one for the non rotating molecule. This may be due to the fact that the reaction mechanism is going through many resonances, thereby dynamically loosing the effects of having "hot" reactants.

Furthermore, by looking at the final distributions over the vibrational channels we have seen that the reaction can easily produce vibrationally excited molecules and the reactive flux is more or less equally redistributed over all the open, final vibrational states. The final rotational populations, as far as we can judge from our data, seem to be strongly dependent on the collision energy and do not show any simple pattern of interpretation.

We have also performed fully converged calculations for  $J = 1$  and  $J = 2$  and we have seen that the latter data provide very similar results to  $J = 0$  calculation although the resonance patterns slightly change and shift in energy, as one expects from such systems. We have thus been able to provide rate constants for the reaction through the use of a  $l$ -shifting approximation [1] which yields final rates of the order of  $10^{-10} \text{ cm}^3 \cdot \text{s}^{-1}$ . The latter results indicate that in the present system the reactive process may be as efficient as the inelastic vibrational de-excitation process estimated earlier by us [8] in providing a mechanism of energy exchange in the droplets. The size of the exchange rate also suggest that observation of such reaction may be possible in the droplet environment.

### Acknowledgments

The financial support of the Scientific Committee of the University of Rome, of the CASPUR Supercomputing Center and of the INTAS grant n. 03-51-6170 is gratefully acknowledged. M.L. thanks the "cold molecules" TRN n. HPRN-CT-2002-00290 for supporting his stay in Rome, where this work begun. The financial support of the same RTN "cold molecules" is also acknowledged.

- 
- [1] S. K. Gray , E. M. Golfield, G. C. Shatz and G. G. Balin-Kurti *Phys. Chem. Chem. Phys.*, **1**, 1141 (1999)
  - [2] J.P. Toennies and A. Vilesov, *Ang. Chem., Int. Ed.*, **43**, 2622, (2004)
  - [3] J.P. Toennies and A. Vilesov, *Ann. Rev. Phys. Chem.* **49**, 1 (1988).

- [4] D. Lopez-Durán, M. P. de Lara-Castels, G. Delgado-Barrio, P. Villarreal, C. Di Paola, F.A. Gianturco, *Phys. Rev. Lett.* **93**, 053401 (2004).
- [5] J.A. Northby, *J. Chem. Phys.* **115**, 10065 (2001).
- [6] D.S. Petereka, A. Lindinger, L. Poisson, M. Ahmed and D.M. Neumark, *Phys. Rev. Lett.* **91**, 043401 (1991).
- [7] H. Buchenan, J.P. Toennies and J. Northby, *J. Chem. Phys.* **95**, 8134 (1991).
- [8] E. Scifoni, G. Delle Piane and F.A. Gianturco, *Eur. Phys. J. D* **30**, 353 (2004).
- [9] E. Scifoni, E. Bodo, G. Delle Piane and F.A. Gianturco, *Eur. Phys. J. D* **30**, 363 (2004).
- [10] M. Lara, A. Aguado, M. Paniagua and O. Roncero, *J. Chem. Phys.*, **113**, 1781 (2000).
- [11] T. Ruchti, K. Förde, B.E. Colliccoat, H. Ludwigs and K.C. Janda, *J. Chem. Phys.* **109**, 10679 (1998).
- [12] M. Fárnik and J.P. Toennies, *J. Chem. Phys.* **118**, 4176 (2003).
- [13] M. Fárnik and J.P. Toennies, *J. Chem. Phys.* **122**, 014307 (2005).
- [14] E. Scifoni, E. Bodo and F.A. Gianturco, *J. Chem. Phys.* **122**, 224312 (2005).
- [15] R. N. Zare, "Angular Momentum", J. Wiley and Sons, Inc. (1998)
- [16] H. Tal-Ezer and R. Kosloff, *J. Chem. Phys.* **81**, 3967 (1984)
- [17] R. Kosloff, *J. Phys. Chem.* **92**, 2087 (1988)
- [18] J.C. Light, I.P. Hamilton and J.V. Lill, *J. Chem. Phys.* **82**, 1400 (1985)
- [19] A.C. Peet and W. Yang, *J. Chem. Phys.* **91**, 6598 (1989)
- [20] J. T. Muckerman, *Chem. Phys. Lett.* **173**, 200 (1990)
- [21] G.C. Corey, J.W. Tromp and D. Lemoine, in "Numerical grid methods and their application to Schrödinger equation", edited by C. Cerjan, Kluwer Academic, New York, (1993)
- [22] O. A. Sharafeddin and J.C. Light, *J. Chem. Phys.* **102**, 3622 (1995)
- [23] O. Roncero, D. Caloto, K.C. Janda and N. Halberstadt, *J. Chem. Phys.* **107**, 1406, (1997)
- [24] G. G. Balint-Kurti, R. N. Dixon, and C. C. Marston, *J. Chem. Soc., Faraday Trans.* **86**, 1741 (1990)
- [25] G. G. Balint-Kurti, F. Göötas, S. P. Mort, A. R. Offer, A. Lagan and O. Gervasi, *J. Chem. Phys.* **99**, 9567 (1993). *J. Chem. Phys.* **113**, 1781 (2000)
- [26] D. Skouteris, J. F. Castillo, D. E. Manolopoulos, *Comp. Phys. Comm.* **133** (2000) 128.
- [27] R. T. Pack, G. A. Parker, *J. Chem. Phys.* **87** (1987) 3888.
- [28] G. C. Shatz, *Chem. Phys. Lett.* **150** (1988) 92.

- [29] G. A. Parker, R. T. Pack, J. Chem. Phys. **98** (1993) 6883.
- [30] D. E. Manolopoulos, J. Chem. Phys. **85** (1986) 6425.